7

Throughput Analysis of Wireless Sensor Networks via Evaluation of Connectivity and MAC performance

Flavio Fabbri and Chiara Buratti
WiLAB, IEIIT-BO/CNR, DEIS University of Bologna
ITALY

1. Introduction

The data throughput that a wireless sensor network (WSN) can guarantee is influenced by a plethora of concurrent causes. Among those, limited connectivity and medium access control (MAC) failures are major issues that should be carefully considered. The aim of this chapter is to provide the reader with a neat and general mathematical framework for the analytical computation of key performance metrics of WSNs. The focus is on connectivity and MAC issues. Quantitative answers to such questions as the following will be given: how well is the network -or a subset of it- connected? What is the rate at which sensors are able to transmit their data to sink(s)? What is the overall throughput of a sensor network deployed on a specific domain?

We consider a multi-sink WSN where sensor and sink nodes are both randomly deployed on a finite or infinite domain. Sensors are in charge of sampling the surrounding environment and send their data to one of the sinks, possibly the one providing the best signal strength. The computation requires some basic assumptions that hold throughout the chapter: two nodes are considered connected if the path loss (including both a deterministic distance-dependent component and a random fluctuation) is above a fixed threshold; all nodes employ the same transmission power; sinks have an ideal connection to an infrastructured processing center.

We first address connectivity issues by considering single-hop networks with nodes deployed on the infinite plane, then, after discussing the role of border effects and providing a mathematical means to deal with them, we consider networks on finite regions of square shape. The probabilities that a randomly chosen sensor is connected to one of the sinks, that all sensors -or some percentage of them- are connected, are computed. The connectivity model is then generalized to handle the case of rectangular deployment regions as well as inhomogeneous nodes densities. However, signal strength based connectivity is not exhaustive for real-life applications where failures may occur due to packet collisions, even in perfect channel conditions. For this reason, we also present a rigorous approach for modeling the MAC layer under a carrier-sense multiple access with collision avoidance (CSMA/CA) protocol when several sensor nodes compete for accessing the same channel at the same time. In particular, the analysis is carried out in the specific case of IEEE 802.15.4 MAC algorithm under both Beacon- and Non Beacon-Enabled operation modes. By looking at a single sink scenario with a number of

sensors, the practical outcome is the probability of successful packet reception by the sink, used to derive the throughput from sensors to sink.
Finally, going back to a multi-sink scenario, we now have the means for computing the probabilities that a sensor is connected to an arbitrary sink and that it succeeds in transmitting its packet. Therefore, by integrating the two building blocks mentioned before, we end up with an analytical tool for studying the performance of multi-sink WSNs, where MAC and connectivity issues are taken into account. Network performance is synthesized by introducing the concept of Area Throughput, that is, the number of samples per unit of time successfully delivered by the sensors to the infrastructure. Numerical results are given for the case of IEEE 802.15.4 MAC protocol. The model is also applicable to WSNs employing any MAC protocol.
The chapter is organized as follows. In Section 2 the application scenario is described and some related works are presented. Section 3 introduces the link and connectivity models used. In Sections 4 and 5 connectivity results are derived for the case of unbounded and bounded networks, respectively. Section 6 is devoted to the MAC model and finally Section 7 reports throughput results.

2. Application Scenario

A multi-sink WSN is considered where data collection from the environment is performed by sampling some physical entities and sending them to some external user. The reference application is spatial/temporal process estimation Verdone et al. (2008) and the environment is observed through queries/response mechanisms: queries are periodically generated by the sinks, and sensor nodes respond by sampling and sending data. Through a simple polling model, sinks periodically issue queries, causing all sensors perform sensing and communicating their measurement results back to the sinks they are associated with. The user, by collecting samples taken from different locations, and observing their temporal variations, can estimate the realisation of the observed process. Good estimates require sufficient data taken from the environment. Often, the data must be sampled from a specific portion of space, even if the sensor nodes are distributed over a larger area. Therefore, only a location-driven subset of sensor nodes must respond to queries. The aim of the query/response mechanism is then to acquire the largest possible number of samples from the area. Since the acquisition of samples from the target area is the main issue for the application scenario considered, a new metric for studying the behavior of the WSN, namely the *Area Throughput*, denoting the amount of samples per unit of time successfully transmitted to the final user originating from the target area, is defined. As expected, area throughput is larger if the density of sensor nodes is larger; on the other hand, if a contention-based MAC protocol is used, the density of nodes significantly affects the ability of the protocol to avoid packet collisions (i.e., simultaneous transmissions from separate sensors toward the same sink). In fact, if the number of sensor nodes per cluster is very large, collisions and backoff procedures can make data transmission impossible under time-constrained conditions, and samples taken from sensors do not reach the sinks and, consequently, the final user. Therefore, the optimization of the area throughput requires proper dimensioning of the density of sensors, in a framework model where both MAC and connectivity issues are considered. Although our model could be applied to any MAC protocol, we particularly refer to CSMA-based protocols, and specifically to IEEE 802.15.4 air interface. In this case, sinks act as PAN coordinators periodically transmitting queries to sensors and waiting for replies. According to the standard, the different personal area network (PAN) coordinators, and therefore the PANs, use different frequency

channels. Therefore no collisions may occur between nodes belonging to different PANss; however, nodes belonging to the same PANs compete when trying to transmit their packets to the sink. An infinite area where sensors and sinks are uniformly distributed at random, is considered. Then, a specific portion of space, of finite size and given shape (without loss of generality, we consider a square or a rectangle), is considered as target area (see Figure 1).

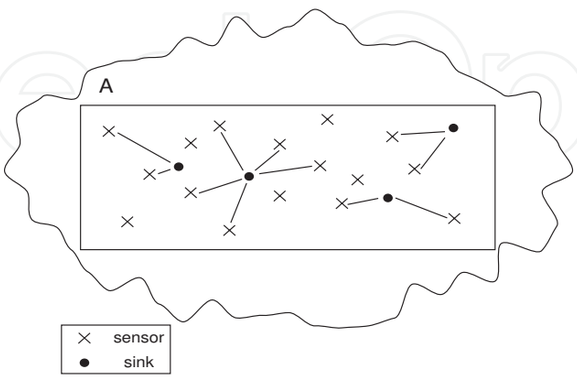

Fig. 1. The Reference Scenario considered.

We assume that sensors and sinks are distributed over the bi-dimensional plane with densities ρ_s and ρ_0, respectively, with the latter much smaller than the former. Denoting with A the area of the target domain and by k the number of sensor nodes in A, k is Poisson distributed with mean $\bar{k} = \rho_s \cdot A$ and p.d.f.

$$g_k = \frac{\bar{k}^k e^{-\bar{k}}}{k!}. \tag{1}$$

We also let $I = \rho_0 \cdot A$ be the average number of sinks in A.
The frequency of the queries transmitted by the sinks is denoted as $f_q = 1/T_q$. Each sensor takes, upon reception of a query, one sample of a given phenomenon and forwards it through a direct link to the sink. Once transmission is performed, it switches to an idle state until reception of the next query. We denote the interval between two successive queries as *round*. The amount of samples available from the sensors deployed in the area, per unit of time, is denoted as *Available Area Throughput*. In this Chapter we determine how the area throughput depends on the available area throughput for different scenarios and system parameters.

2.1 Related Works

Many works in the literature devoted their attention to connectivity in WSNs or to the analytical study of carrier-sense multiple access (CSMA)-based MAC protocols. However, very few papers jointly consider the two issues under a mathematical approach. Some analysis of the two aspects are performed through simulations: as examples, Stuedi et al. (2005) related to ad hoc networks, and Buratti & Verdone (2006), to WSN. Many papers based on random graph theory, continuum percolation and geometric probability Bollobàs (2001); Meester & Roy (1996); Penrose (1993; 1999); Penrose & Pistztora (1996) addressed connectivity issues of networks. In particular, wireless ad hoc and sensor networks have recently attracted a growing attention Bettstetter (2002); Bettstetter & Zangl (2002); Pishro-Nik et al. (2004); Salbaroli & Zanella (2006); Santi & Blough (2003); Vincze et al. (2007). A great insight on connectivity of ad hoc wireless networks is provided in Bettstetter (2002); Bettstetter & Zangl (2002); Santi & Blough (2003). Nonetheless, the authors do not account for random channel fluctuations and

do not explicitly discuss the presence of one or more fusion centers (sinks) in the given region. Connectivity-related issues of WSNs are addressed in Salbaroli & Zanella (2006); Vincze et al. (2007). In Salbaroli & Zanella (2006), while considering channel randomness, the authors restrict the analysis to a single-sink scenario. Although single-sink scenarios have attracted more attention so far, multi-sink networks have been increasingly considered in the very recent time. As an example, Vincze et al. (2007) addresses the problem of deploying multiple sinks in a multi-hop limited WSN. However, the work presents a deterministic approach to distribute the sinks on a given region, rather than considering a more general uniform random deployment. Furthermore, since the finiteness of deployment region plays a not secondary role on connectivity, those models based on bounded domains turn out to be of more practical use.

Concerning the analytical study of CSMA-based MAC protocols, in Takagi & Kleinrock (1985) the throughput for a finite population when a persistent CSMA protocol is used, is evaluated. An analytical model of the IEEE 802.11 CSMA-based MAC protocol, is presented by Bianchi in Bianchi (2000). In these works no physical layer or channel model characteristics are accounted for. Capture effects with CSMA in Rayleigh channels are considered in Zdunek et al. (1989), whereas Kim & Lee (1999) addresses CSMA/CA protocols. However, no connectivity issues are considered in these papers: the transmitting terminals are assumed to be connected to the destination node. In Siripongwutikorn (2006) the per-node saturated throughput of an IEEE 802.11b multi-hop ad hoc network with a uniform transmission range, is evaluated under simplified conditions from the viewpoint of channel fluctuations and number of nodes. Also, some studies have tried to describe analytically the behavior of the 802.15.4 MAC protocol. Few works devoted their attention to non beacon-enabled mode (see, e.g. Kim et al. (2006)); most of the analytical models are related to beacon-enabled networks Misic et al. (2004; 2005; 2006); Park et al. (2005); Pollin et al. (2008). Some of these fail to match simulation results (see, e.g. Pollin et al. (2008)), whereas slightly more accurate models are proposed in Park et al. (2005) and Chen et al. (2007), where, however, the sensing states are not correctly captured by the Markov chain. In conclusion, the most relevant difference between the previously cited models and the one developed in Buratti & Verdone (2009) and Buratti (2009) and used here, is that the latter precisely captures the algorithm defined by the standard, while considering a typical WSN scenario. In our scenario nodes only have one packet to transmit to the sink (i.e., when they receive the query and have to transmit data before the reception of the subsequent query). Therefore, the number of nodes competing for channel at a given time is unknown and not constant (as it is in the above cited works) but it decreases with time, since successful nodes go to sleep till next query.

Finally, to the best of the Authors knowledge, no one has so far introduced any connectivity/MAC model for WSNs while jointly considering the following aspects: presence of both sensors and multiple sinks, random deployment of nodes, bounded scenarios, channel fluctuations, realistic MAC protocol in non-saturation condition.

3. Link and Connectivity Models

Many works in the WSN scientific literature assume deterministic distance- dependent and threshold-based packet capture models. This means that all nodes within a circle centered at the transmitter can receive a packet sent by the transmitting one Bettstetter (2002); Bettstetter & Zangl (2002); Santi & Blough (2003). While the threshold-based capture model, which assumes that a packet is captured if the signal-to-noise ratio (in the absence of interference) is above a given threshold, is a good approximation of real capture effects, the deterministic

channel model does not represent realistic situations in most cases. The use of realistic channel models is therefore of primary importance in wireless systems.
In this chapter, a narrow-band channel, accounting for the power loss due to propagation effects including a distance-dependent path loss and random channel fluctuations, is considered.
Specifically, the power loss in decibel scale at distance d is expressed in the following form

$$L(d) = k_0 + k_1 \ln d + s, \tag{2}$$

where k_0 and k_1 are constants, s is a Gaussian r.v. with zero mean, variance σ^2, which represents the channel fluctuations. This channel model was also adopted by Orriss and Barton Orriss & Barton (2003) and other Authors Miorandi & Altman (2005). In Verdone et al. (2008) experimental measurement results, performed with 802.15.4 devices at 2.4 [GHz] Industrial Scientific Medical (ISM) band, deployed in different environments (grass, asphalt, indoor, etc), are shown. It is found for the received power in logarithmic scale that in general a Gaussian model can approximate the measurement variation fairly well, with different values of the standard deviation. By suitably setting k_1, it is possible to accommodate an inverse square law relationship between power and distance ($k_1 = 8.69$), or an inverse fourth-power law ($k_1 = 17.37$), as examples.
For what concerns the link model, a radio link between two nodes is said to exist, which means that the two nodes are *connected* or *audible* to each other [1], if $L < L_{th}$, where L_{th} represents the maximum loss tolerable by the communication system. The threshold L_{th} depends on the transmit power and the receiver sensitivity.
By solving (2) for the distance d with $L = L_{\text{th}}$, we can define the transmission range

$$TR = e^{\frac{L_{\text{th}} - k_0 - s}{k_1}}, \tag{3}$$

as the maximum distance between two nodes at which communication can still take place. Such range defines the connectivity region of the sensor. Note that by adopting independent r.v.'s s for separate links, we have different values of TR for different sinks, given a generic sensor. In other words, unlike many papers dealing with connectivity issues in the literature Bettstetter (2002); Bettstetter & Zangl (2002); Santi & Blough (2003), we do not use circles to predict sensor connectivity. However, by setting $\sigma = 0$, we neglect the channel fluctuations and may still define an ideal transmission range, as a reference, as

$$TR_{\text{i}} = e^{\frac{L_{\text{th}} - k_0}{k_1}}. \tag{4}$$

Finally, we can define a connection function between any node pair whose distance is d as

$$g(d) = \text{Prob}\left\{L(d) < L_{\text{th}}\right\} = 1 - \frac{1}{2}\text{erfc}\left(\frac{L_{\text{th}} - k_0 - k_1 \ln d}{\sqrt{2}\sigma}\right). \tag{5}$$

3.1 Connectivity properties in Poisson fields

Connectivity theory studies networks formed by large numbers of nodes distributed according to some statistics over a limited or unlimited region of $\mathbb{R}^d$, with d=1,2,3, and aims at describing the potential set of links that can connect nodes to each other, subject to some constraints from the physical viewpoint (power budget, or radio resource limitations).

[1] link's reciprocity is assumed.

It is widely accepted that, a WSN is *fully-connected* in case any sensor node is able to reach at least one sink node, either directly or through other sensor nodes Verdone et al. (2008) (not necessarily requiring any node to be reached by any other node).
Let us consider a stationary Poisson Point Process (PPP) $\Phi = \{\mathbf{x_1}, \mathbf{x_2}, \ldots\}$ having intensity ρ, with $\mathbf{x_i} = (x_i, y_i)$, $i = 1, 2, \ldots$ being a random point in $\mathbb{R}^2$. Φ may also be regarded as a random measure on the Borel sets in $\mathbb{R}^2$: taken any $\Omega \subset \mathbb{R}^2$ having area W_Ω, $\Phi(\Omega)$ is a Poisson r.v. which counts the number of points of Φ that lie in the set Ω, whose first order moment is

$$\mathbf{E}(\Phi(\Omega)) = \rho \nu_d(\Omega) = \rho \int_\Omega d\mathbf{x} = \rho W_\Omega, \tag{6}$$

where $\nu_d(\Omega)$ is the Lebesgue measure of Ω. Now suppose we want to count only those points in Ω which are connected to an arbitrary node $\mathbf{x_0}$: this implies a thinning procedure on Φ such that each point is retained with probability $C(||\mathbf{x_0} - \mathbf{x_i}||)$ and discarded with probability $1 - C(||\mathbf{x_0} - \mathbf{x_i}||)$, $i = 1, 2, \ldots$, where $C(x)$ is a non-negative measurable function such that $0 \leq C(x) \leq 1$. By so doing, the new inhomogeneous process Φ' is obtained.
By recalling the *Campbell Theorem* for point processes Gardner (1989) that we report for later use

$$\mathbf{E}\left(\sum_{\mathbf{x}\in\Omega} f(\mathbf{x})\right) = \rho \int_\Omega f(\mathbf{x}) d\mathbf{x}, \tag{7}$$

for any non-negative measurable function f, we have for Φ'

$$\mu = \mathbf{E}(\Phi'(\Omega)) = \mathbf{E}\left(\sum_{\mathbf{x}\in\Omega} C(||\mathbf{x_0} - \mathbf{x}||)\right) = \rho \int_\Omega C(||\mathbf{x_0} - \mathbf{x}||) d\mathbf{x}. \tag{8}$$

In particular, when the channel model of eq. (2) is used (i.e., $C(x) \equiv g(x)$), the mean number of nodes audible within a range of distances r_1 and r, to a generic node ($r \geq r_1$), is denoted as $\mu_{r_1,r}$ and can be written as Orriss & Barton (2003); Orriss et al. (1999)

$$\mu_{r_1,r} = \pi\rho[\Psi(a_1, b_1; r) - \Psi(a_1, b_1; r_1)], \tag{9}$$

where ρ is the initial nodes' density and

$$\begin{aligned} \Psi(a_1, b_1; r) &= r^2 \Phi(a_1 - b_1 \ln r) \\ &- e^{\frac{2a_1}{b_1} + \frac{2}{b_1^2}} \Phi(a_1 - b_1 \ln r + 2/b_1), \end{aligned} \tag{10}$$

and $a_1 = (L_{\text{th}} - k_0)/\sigma$, $b_1 = k_1/\sigma$ and $\Phi(x) = \int_{-\infty}^{x} (1/\sqrt{2\pi}) e^{-u^2/2} du$.

4. Connectivity in Unbounded Networks

Since the channel model described by eq. (2) is used, the number of audible sinks within a range of distances r_1 and r from a generic sensor node ($r \geq r_1$), $n_{r_1,r}$, is Poisson distributed with mean $\mu_{r_1,r}$, given by eq. (9) by simply substituting ρ with ρ_0. Then by letting $r_1 = 0$ and $r \to \infty$, we obtain

$$\mu_{0,\infty} = \pi\rho_0 \exp[(2(L_{\text{th}} - k_0)/k_1) + (2\sigma^2/k_1^2)]\,. \tag{11}$$

Equation (11) represents the mean value of the total number, $n_{0,\infty}$, of audible sinks for a generic sensor, obtained considering an infinite plane Orriss & Barton (2003).
Its non-isolation probability is simply the probability that the number of audible sinks is greater than zero

$$q_\infty = 1 - e^{-\mu_{0,\infty}}. \tag{12}$$

5. Connectivity in Bounded Networks

When moving to networks of nodes located in bounded domains, two important changes happen. First, even with ρ_0 unchanged, the number of sinks that are audible from a generic sensor will be lower due to geometric constraints (a finite area contains (on average) a lower number of audible sinks than an infinite plane). Second, the mean number of audible sinks will depend on the position (x, y) in which the sensor node is located in the region that we consider. The reason for this is that sensors which are at a distance d from the border, with $d \sim TR_{\mathrm{i}}$, have smaller connectivity regions and thus the average number of audible sinks is smaller. These effects, known in literature as *border effects* Bettstetter & Zangl (2002), are accounted for in our model.
The result (9) can be easily adjusted to show that the number of audible sinks within a sector of an annulus having radii r_1 and r and subtending an angle 2θ, is once again Poisson distributed with mean

$$\mu_{r_1,r;\theta} = \theta\rho_0[\Psi(a_1, b_1; r) - \Psi(a_1, b_1; r_1)], \tag{13}$$

$0 \leq \theta \leq \pi$. If the annulus extends from r to $r + \delta r$, and $\theta = \theta(r)$, this mean value becomes

$$\mu_{r,r+\delta r;\theta} = \theta(r)\rho_0 \frac{\delta\Psi(a_1, b_1; r)}{\delta r}\delta r,\ 0 \leq \theta \leq \pi. \tag{14}$$

Consider now a polar coordinate system whose origin coincides with a sensor node. As a consequence of (14), if a region is located within the two radii r_1 and r_2 and its points at a distance r from the origin are defined by a $\theta(r)$ law (see Fabbri & Verdone (2008), Fig. 1), then the number of audible sinks in such a region is again Poisson distributed with mean $\mu_{r_1,r_2;\theta(r)} = \int_{r_1}^{r_2} \theta(r)\rho_0 \frac{d\Psi(a_1,b_1;r)}{dr} dr$, that is, from (10) and after some algebra,

$$\mu_{r_1,r_2;\theta(r)} = \int_{r_1}^{r_2} 2\theta(r)\rho_0 r\Phi(a_1 - b_1 \ln r)dr. \tag{15}$$

5.1 Square Regions

Now consider a square SA of side L meters and area $A = L^2$, sensors and sinks uniformly distributed on it with densities ρ_s and ρ_0, respectively. Equation (15) is suitable for expressing the mean number of audible sinks from an arbitrary point (x, y) of SA, provided that such point is considered as a new origin and that the boundary of SA is expressed with respect to the new origin as a function of r_1, r_2 and $\theta(r)$. In order to apply equation (15) to this scenario and obtain the mean number, $\mu(x, y)$, of audible sinks from the point (x, y), it is needed to set the origin of a reference system in (x, y), partition SA in eight subregions ($S_{\mathrm{r},1} \ldots S_{\mathrm{r},8}$) by means of circles whose centers lie in (x, y) (see Fabbri & Verdone (2008), Fig. 2). Thank to the properties of Poisson r.v.'s, the contribution of each region can be summed and we obtain an exact expression for

$$\mu(x, y) = \sum_{i=1}^{8} \int_{r_{1,i}}^{r_{2,i}} 2\theta_i(r) \cdot \rho_0 \cdot r \cdot \Phi(a_1 - b_1 \ln r)dr, \tag{16}$$

which is the mean number of sinks in SA that are audible from (x, y), where $r_{1,i}$, $r_{2,i}$, $\theta_i(r)$ are reported in Fabbri & Verdone (2008), Tables 1-2.

If we assume a single-hop network, a sensor potentially located in (x, y) is isolated (i.e., there are no audible sinks from its position) with probability $p(x, y) = e^{-\mu(x,y)}$ and it is non isolated with probability

$$q(x, y) = 1 - e^{-\mu(x,y)}. \tag{17}$$

Owing to the assumption that sensor nodes are uniformly and randomly distributed in SA, if we now want to compute the probability that a randomly chosen sensor node is not isolated, we need to take the average $q(x, y)$ on SA. In fact, the probability that a randomly chosen sensor node is not isolated (which is an ensemble measure) and the average non-isolation probability over a single realization coincides due to the ergodicity of stationary Poisson processes (see Stoyan et al. (1995), page 104). This was also verified by simulation.
Recalling that we have considered the lower half of the first quadrant, which is one eighth of the totality, we have

$$\overline{q} = \frac{8}{A} \int_0^{L/2} \int_0^x q(x, y) dy dx. \tag{18}$$

5.2 Rectangular Regions

We now consider a rectangular domain $\mathcal{C}$ of sides S_1 and S_2, $S_1 > S_2$, area $W = S_1 \cdot S_2$, with sensors and sinks uniformly distributed on it with densities ρ_s and ρ_0, respectively. We aim at computing the mean number of audible sinks from a fixed position (x, y) which are contained in $\mathcal{C}$. Since we are dealing with a rectangular domain whose points have to be expressed in polar coordinates in order to apply (15), such a domain has to be properly partitioned into a set of subregions, to be defined in terms of r_1, r_2, and θ. Moreover, unlike the case of square domain, the nature of the partition depends on the position (x, y) considered. In particular, if we restrict the analysis to the upper-right quart, we can identify 4 different cases depending on whether (x, y) belongs to A_1, A_2, A_3 or A_4 (see Figure 2). Let us denote as *case i* the event $(x, y) \in A_i$, for $i = 1, 2, 3, 4$. In each of the latter cases, the domain is differently partitioned into 8 subregions that are sectors of annuli. What changes from one case to another is the definition of each subregion. As an example, the subregion having r in the range $[0, S_1/2 - y[$ lies completely in $\mathcal{C}$ only when $(x, y) \in A_2$; otherwise it partially exceeds the borders of $\mathcal{C}$. Thus, the corresponding angle $\theta(r)$ is π in case 2 and some function of r in the other cases. The following tables define A_1-A_4 and the values of r and θ in each subregion for case $i = 1, 2, 3, 4$, respectively. In the following, we denote by $[r_{1,j}^{(A_i)}, r_{2,j}^{(A_i)}[$ the range of r of the jth subregion when in case i, and by $\theta_j^{(A_i)}(r)$ the corresponding angle.

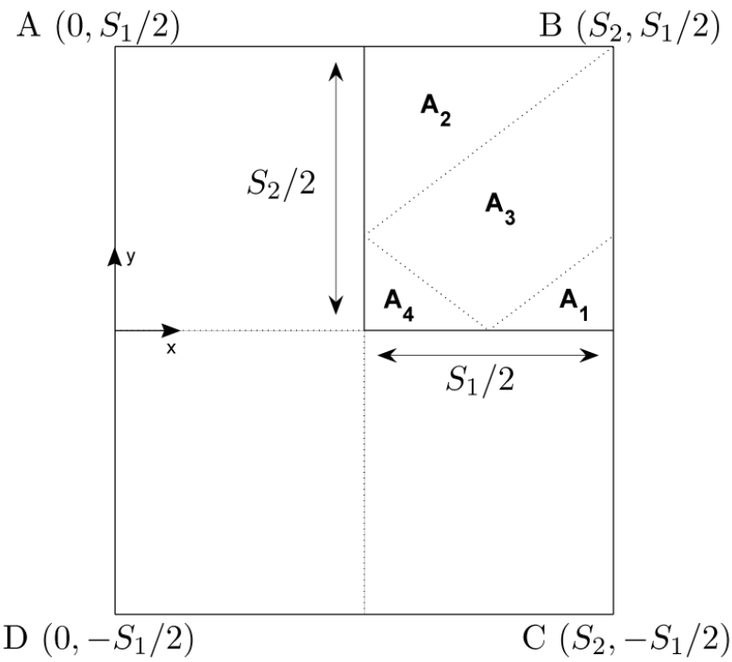

Fig. 2. Geometric partitioning of the rectangular region.

Case	Definition
A_1	$(x,y) \mid \{S_1/2 \le x \le S_2,\ \ 0 \le y \le x - S_1/2\}$
A_2	$(x,y) \mid \{S_2/2 \le x \le S_2,\ \ x + S_1/2 - S_2 \le y \le S_1/2\}$
A_3	$(x,y) \mid \{S_2/2 \le x \le S_2,\ \ \max(S_1/2 - x, x - S_1/2) \le y \le S_1/2 - S_2 + x\}$
A_4	$(x,y) \mid \{S_2/2 \le x \le S_1/2,\ \ 0 \le y \le S_1/2 - x\}$

Region	Range: $r_1^{(A_1)} \le r < r_2^{(A_1)}$	$\theta^{(A_1)}(r)$
1	$0 \le r < S_2 - x$	π
2	$S_2 - x \le r < S_1/2 - y$	$\frac{\pi}{2} + \arcsin \frac{S_2 - x}{r}$
3	$S_1/2 - y \le r < \sqrt{(S_2 - x)^2 + (S_1/2 - y)^2}$	$\frac{\pi}{2} + \arcsin \frac{S_1/2 - y}{r} - \arccos \frac{S_2 - x}{r}$
4	$\sqrt{(S_2 - x)^2 + (S_1/2 - y)^2} \le r < S_1/2 + y$	$\frac{\pi}{2} + \frac{1}{2}\left(\arcsin \frac{S_2 - x}{r} - \arccos \frac{S_1/2 - y}{r}\right)$
5	$S_1/2 + y \le r < \sqrt{(S_2 - x)^2 + (S_1/2 + y)^2}$	$\frac{\pi}{2} - \arccos \frac{S_1/2 + y}{r} + \frac{1}{2}\left(\arcsin \frac{S_2 - x}{r} - \arccos \frac{S_1/2 - y}{r}\right)$
6	$\sqrt{(S_2 - x)^2 + (S_1/2 + y)^2} \le r < x$	$\frac{\pi}{2} - \frac{1}{2}\left(\arccos \frac{S_1/2 + y}{r} + \arccos \frac{S_1/2 - y}{r}\right)$
7	$x \le r < \sqrt{x^2 + (S_1/2 - y)^2}$	$\frac{1}{2}\left(\arcsin \frac{S_1/2 - y}{r} + \arcsin \frac{S_1/2 + y}{r}\right) - \arccos \frac{x}{r}$
8	$\sqrt{x^2 + (S_1/2 - y)^2} \le r < \sqrt{x^2 + (S_1/2 + y)^2}$	$\frac{1}{2}\left(\arcsin \frac{S_1/2 + y}{r} - \arccos \frac{x}{r}\right)$

Region	Range: $r_1^{(A_2)} \le r < r_2^{(A_2)}$	$\theta^{(A_2)}(r)$
1	$0 \le r < S_1/2 - y$	π
2	$S_1/2 - y \le r < S_2 - x$	$\frac{\pi}{2} + \arcsin \frac{S_1/2 - y}{r}$
3	$S_2 - x \le r < \sqrt{(S_2 - x)^2 + (S_1/2 - y)^2}$	$\frac{\pi}{2} + \arcsin \frac{S_1/2 - y}{r} - \arccos \frac{S_2 - x}{r}$
4	$\sqrt{(S_2 - x)^2 + (S_1/2 - y)^2} \le r < x$	$\frac{\pi}{2} + \frac{1}{2}\left(\frac{S_1/2 - y}{r} - \arccos \frac{S_2 - x}{r}\right)$
5	$x \le r < \sqrt{x^2 + (S_1/2 - y)^2}$	$\frac{\pi}{2} - \arccos \frac{S_1/2 + y}{r} + \frac{1}{2}\left(\arcsin \frac{S_1/2 + y}{r} - \arccos \frac{S_2 - x}{r}\right)$
6	$\sqrt{x^2 + (S_1/2 - y)^2} \le r < S_1/2 + y$	$\frac{1}{2}\left(\arcsin \frac{S_2 + x}{r} + \arcsin \frac{x}{r}\right)$
7	$S_1/2 + y \le r < \sqrt{(S_2 - x)^2 + (S_1/2 + y)^2}$	$\frac{1}{2}\left(\arcsin \frac{x}{r} + \arcsin \frac{S_2 - x}{r}\right) - \arccos \frac{S_1/2 + y}{r}$
8	$\sqrt{(S_2 - x)^2 + (S_1/2 + y)^2} \le r < \sqrt{x^2 + (S_1/2 + y)^2}$	$\frac{1}{2}\left(\arcsin \frac{x}{r} - \arccos \frac{S_1/2 + y}{r}\right)$

Region	Range: $r_1^{(A_3)} \leq r < r_2^{(A_3)}$	$\theta^{(A_3)}(r)$
1	$0 \leq r < S_2 - x$	π
2	$S_2 - x \leq r < S_1/2 - y$	$\frac{\pi}{2} + \arcsin \frac{S_2 - x}{r}$
3	$S_1/2 - y \leq r < \sqrt{(S_2 - x)^2 + (S_1/2 - y)^2}$	$\frac{\pi}{2} + \arcsin \frac{S_1/2 - y}{r} - \arccos \frac{S_2 - x}{r}$
4	$\sqrt{(S_2 - x)^2 + (S_1/2 - y)^2} \leq r < x$	$\frac{\pi}{2} + \frac{1}{2}\left(\arcsin \frac{S_1/2 - y}{r} - \arccos \frac{S_2 - x}{r}\right)$
5	$x \leq r < \sqrt{x^2 + (S_1/2 - y)^2}$	$\frac{\pi}{2} - \arccos \frac{S_1/2 + y}{r} + \frac{1}{2}\left(\arcsin \frac{S_1/2 - y}{r} - \arccos \frac{S_2 - x}{r}\right)$
6	$\sqrt{x^2 + (S_1/2 - y)^2} \leq r < S_1/2 + y$	$\frac{\pi}{2} - \frac{1}{2}\left(\arccos \frac{x}{r} + \arccos \frac{S_2 - x}{r}\right)$
7	$S_1/2 + y \leq r < \sqrt{(S_2 - x)^2 + (S_1/2 + y)^2}$	$\arcsin \frac{S_1/2 + y}{r} - \frac{1}{2}\left(\arccos \frac{S_2 - x}{r} + \arccos \frac{x}{r}\right)$
8	$\sqrt{(S_2 - x)^2 + (S_1/2 + y)^2} \leq r < \sqrt{x^2 + (S_1/2 + y)^2}$	$\frac{1}{2}\left(\arcsin \frac{x}{r} - \arccos \frac{S_1/2 + y}{r}\right)$

Region	Range: $r_1^{(A_4)} \leq r < r_2^{(A_4)}$	$\theta^{(A_4)}(r)$
1	$0 \leq r < S_2 - x$	π
2	$S_2 - x \leq r < x$	$\frac{\pi}{2} + \arcsin \frac{S_2 - x}{r}$
3	$x \leq r < S_1/2 - y$	$\frac{\pi}{2} + \arcsin \frac{S_2 - x}{r} - \arccos \frac{x}{r}$
4	$S_1/2 - y \leq r < \sqrt{(S_2 - x)^2 + (S_1/2 - y)^2}$	$\frac{\pi}{2} + \arcsin \frac{S_1/2 - y}{r} - \arccos \frac{x}{r} - \arccos \frac{S_2 - x}{r}$
5	$\sqrt{(S_2 - x)^2 + (S_1/2 - y)^2} \leq r < \sqrt{x^2 + (S_1/2 - y)^2}$	$\frac{\pi}{2} - \arccos \frac{S_1/2 + y}{r} + \frac{1}{2}\left(\arcsin \frac{S_1/2 - y}{r} - \arccos \frac{S_2 - x}{r}\right)$
6	$\sqrt{x^2 + (S_1/2 - y)^2} \leq r < S_1/2 + y$	$\frac{\pi}{2} - \frac{1}{2}\left(\arccos \frac{S_2 - x}{r} + \arccos \frac{x}{r}\right)$
7	$S_1/2 + y \leq r < \sqrt{(S_2 - x)^2 + (S_1/2 + y)^2}$	$\frac{\pi}{2} - \arccos \frac{S_1/2 + y}{r} - \frac{1}{2}\left(\arccos \frac{x}{r} + \arccos \frac{S_2 - x}{r}\right)$
8	$\sqrt{(S_2 - x)^2 + (S_1/2 + y)^2} \leq r < \sqrt{x^2 + (S_1/2 + y)^2}$	$\frac{1}{2}\left(\arcsin \frac{S_1 + y}{r} - \arccos \frac{x}{r}\right)$

Note that when $S_1 = S_2$ the partitioning scheme degenerates to the one for square regions. Now, starting from (15) and owing to the linearity of Poisson independent r.v.'s, the mean number of sinks that are audible from (x, y), with $(x, y) \in A_i$, may be computed as

$$\mu^{(A_i)}(x, y) = \sum_{j=1}^{8} \int_{r_{1,j}^{(A_i)}}^{r_{2,j}^{(A_i)}} 2\theta_j^{(A_i)}(r) \cdot \rho_0 \cdot r \cdot \Phi(a_1 - b_1 \ln r) dr, \tag{19}$$

for $i = 1, 2, 3, 4$ and with $a_1 = (L_{\text{th}} - k_0)/\sigma$, $b_1 = k_1/\sigma$ and $\Phi(x) = \int_{-\infty}^{x} (1/\sqrt{2\pi}) e^{-u^2/2} du$. Owing to the Poisson distribution of the number of audible sinks, the probability that the position (x, y), with $(x, y) \in A_i$, is isolated (i.e., no sink is heard) is simply

$$p^{(A_i)}(x, y) = e^{-\mu^{(A_i)}(x,y)}, \tag{20}$$

while the probability that the position (x, y), with $(x, y) \in A_i$, is not isolated is

$$q^{(A_i)}(x, y) = 1 - p^{(A_i)}(x, y) = 1 - e^{-\mu^{(A_i)}(x,y)}. \tag{21}$$

Now, the mean number of sinks that are audible from (x, y), with $(x, y) \in \{A_1 \cup A_2 \cup A_3 \cup A_4\}$, is

$$\mu(x, y) = \begin{cases} \mu^{(A_1)}(x, y) & , (x, y) \in A_1 \\ \mu^{(A_2)}(x, y) & , (x, y) \in A_2 \\ \mu^{(A_3)}(x, y) & , (x, y) \in A_3 \\ \mu^{(A_4)}(x, y) & , (x, y) \in A_4 \end{cases} \tag{22}$$

Equally, the isolation and non-isolation probabilities may be computed as

$$p(x, y) = \begin{cases} p^{(A_1)}(x, y) = e^{-\mu^{(A_1)}(x,y)} & , (x, y) \in A_1 \\ p^{(A_2)}(x, y) = e^{-\mu^{(A_2)}(x,y)} & , (x, y) \in A_2 \\ p^{(A_3)}(x, y) = e^{-\mu^{(A_3)}(x,y)} & , (x, y) \in A_3 \\ p^{(A_4)}(x, y) = e^{-\mu^{(A_4)}(x,y)} & , (x, y) \in A_4 \end{cases} \tag{23}$$

and

$$q(x,y) = \begin{cases} q^{(A_1)}(x,y) = 1 - e^{-\mu^{(A_1)}(x,y)} & ,(x,y) \in A_1 \\ q^{(A_2)}(x,y) = 1 - e^{-\mu^{(A_2)}(x,y)} & ,(x,y) \in A_2 \\ q^{(A_3)}(x,y) = 1 - e^{-\mu^{(A_3)}(x,y)} & ,(x,y) \in A_3 \\ q^{(A_4)}(x,y) = 1 - e^{-\mu^{(A_4)}(x,y)} & ,(x,y) \in A_4, \end{cases} \tag{24}$$

respectively. Hence, the average probability of non-isolation over $\mathcal{C}$ is

$$\begin{aligned} \overline{q} &= \mathbb{E}_{x,y}[q(x,y)] = \frac{4}{W}\int_{S_2/2}^{S_2}\int_{0}^{S_1/2} q(x,y)dydx \\ &= \frac{4}{W}\left(\int_{S_1/2}^{S_2}\int_{0}^{x-S_1/2} q^{(A_1)}(x,y)dydx + \int_{S_2/2}^{S_2}\int_{x+S_1/2-S_2}^{S_1/2} q^{(A_2)}(x,y)dydx \right. \\ &\quad + \left. \int_{S_2/2}^{S_2}\int_{\max(S_1/2-x,x-S_1/2)}^{S_1/2-S_2+x} q^{(A_3)}(x,y)dydx + \int_{S_2/2}^{S_1/2}\int_{0}^{S_1/2-x} q^{(A_4)}(x,y)dydx \right) \end{aligned} \tag{25}$$

5.3 Composite Domains

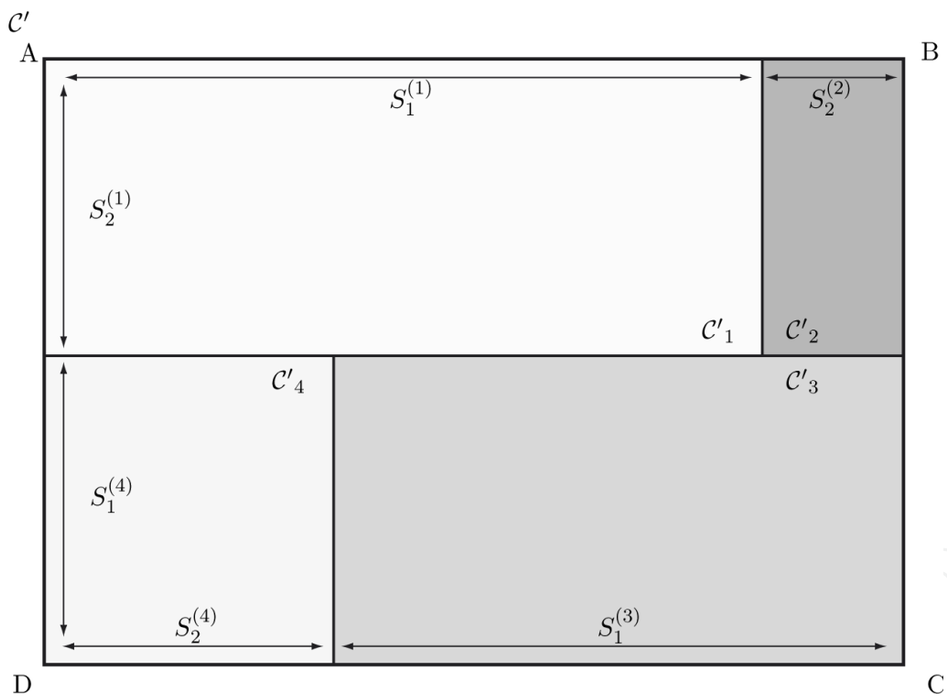

Fig. 3. Reference scenario for the analysis of composite domains.

The scenario that we now want to analyze is of the kind of the one depicted in Figure 3. Consider a rectangular domain $\mathcal{C}'$ of area W' which is composed of n rectangular sub-domains $\mathcal{C}'_i$ of sides $S_1^{(i)}$ and $S_2^{(i)}$ (note that $S_1^{(i)} \geq S_2^{(i)}$ holds), area $W^{(i)}$, $i = 1,2,\ldots,n$. We assume the sinks are uniformly and randomly distributed in $\mathcal{C}'_i$ with density $\rho_{0,i}$, $i = 1,2,\ldots,n$. Instead, sensors are uniformly and randomly distributed over the whole domain (i.e., in $\mathcal{C}'$) with density ρ_s. As a consequence, sinks are distributed according to a inhomogeneous PPP over $\mathcal{C}'$, while sensors are distributed according to a homogeneous PPP over $\mathcal{C}'$.

Our final goal is to compute the probability that a randomly chosen sensor in $\mathcal{C}'$ is not isolated. Now suppose there is a sensor node, S, located in $(S_x, S_y) \in \mathcal{C}'_k$ and we want to find the probability that it is not isolated. It is clear that the number of sinks that S can hear is not limited to the number of sinks contained in $\mathcal{C}'_k$. Rather, the more its transmission range is large compared to the sides of $\mathcal{C}'_k$, the more it can benefit from the connectivity offered by the sinks located in the other sub-domains (e.g., the adjacent ones). On the contrary, when S is not close to one of the borders of $\mathcal{C}'_k$ and its transmission range is small (i.e., the connectivity area of S lies entirely within $\mathcal{C}'_k$), what happens in $\mathcal{C}'_j$, $\forall j \neq k$ is totally negligible. We can intuitively state that the same happens when $\rho_{0,k} \gg \rho_{0,j}$, $\forall j \neq k$, since the other sub-domains present too few sinks to provide connectivity to a sensor in $\mathcal{C}'_k$.
Thus, when we are allowed to neglect the interaction between different sub-domains, we can simply treat each of them in a separate way. In this way we end up with the n-tuple $\bar{\mathbf{q}} = (\bar{q}_1, \bar{q}_2, \ldots, \bar{q}_n)$. The overall approximated non-isolation probability over $\mathcal{C}'$ is obtained as the weighted average of $\bar{\mathbf{q}}$. This case is detailed in Subsection 5.3.1.
As an alternative, a direct application of (8) with a careful choice of Ω (i.e., without partitioning) would lead to an exact result. However, the complexity of carrying out the integration can sometimes make this approach unfeasible. The details can be found in Subsection 5.3.2.

5.3.1 Approach 1

We have $\bar{\mathbf{q}} = (\bar{q}_1, \bar{q}_2, \ldots, \bar{q}_n)$, with (from (25))

$$\bar{q}_i = \mathbb{E}_{x,y}[q_i(x,y)] = \frac{4}{W^{(i)}} \int_{S_2^{(i)}/2}^{S_2^{(i)}} \int_0^{S_1^{(i)}/2} q_i(x,y)\,dy\,dx, \tag{26}$$

where $q_i(x,y)$ is computed on $\mathcal{C}'_i$, which has sides $S_1^{(i)}$ and $S_2^{(i)}$ with $S_1^{(i)} \geq S_2^{(i)}$, $i = 1, 2, \ldots, n$. Now, the probability, $\bar{q}_{\mathrm{P}}$, that a randomly chosen sensor in $\mathcal{C}'$ is not isolated is simply

$$\bar{q}_{\mathrm{P}} = \frac{1}{W'} \sum_{i=1}^{n} W^{(i)} \bar{q}_i. \tag{27}$$

5.3.2 Approach 2

From (8) and owing once again to the fact that the sum of Poisson independent r.v.'s having mean λ_i, $i = 1, 2, \ldots$, is still Poisson with mean $\Lambda = \lambda_1 + \lambda_2 + \ldots$, we have

$$\mu_{\mathrm{M}}(x_0, y_0) = \sum_{k=1}^{n} \rho_{0,k} \int_{\mathcal{C}'_k} C(||\mathbf{x} - \mathbf{x}_0||)\,d\mathbf{x}, \tag{28}$$

i.e., the average number of audible sinks from (x_0, y_0).
Equation (28) is very general and takes the interaction between sub-domains into account. Now, in order to obtain a result which is analogous to (25), we let

$$p_{\mathrm{M}}(x_0, y_0) = e^{-\mu_{\mathrm{M}}(x_0, y_0)} \tag{29}$$

and

$$q_{\mathrm{M}}(x_0, y_0) = 1 - p_{\mathrm{M}}(x_0, y_0) = 1 - e^{-\mu_{\mathrm{M}}(x_0, y_0)} \tag{30}$$

to end up with the isolation and non-isolation probabilities of the location (x_0, y_0), respectively. Then, we simply take the average over the points (x_0, y_0) such that $(x_0, y_0) \in \mathcal{C}'$ and get

$$\bar{q}_{\mathrm{M}} = \frac{1}{W'} \int \int_{\mathcal{C}'} q_{\mathrm{M}}(x_0, y_0)\,dx_0\,dy_0. \tag{31}$$

5.4 Practical Cases With Numerical Results

5.4.1 Single Rectangle

Equation (25) can be evaluated numerically once S_1, S_2, ρ_0, L_{th}, k_0, k_1, σ are known. As an example, in Fig. 4 we plot $\overline{q}$ as a function of the ratio $\gamma = S_2/S_1$.

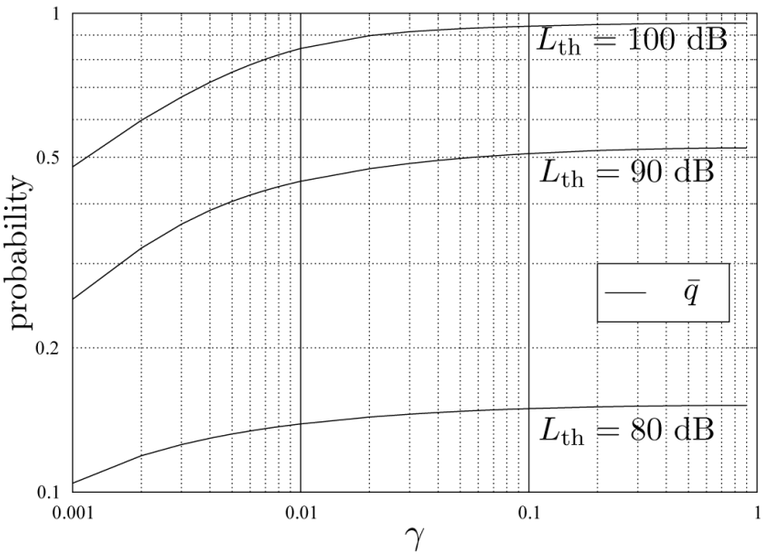

Fig. 4. $\bar{q}$ as a function of γ for different values of $L_{\rm th}$, with $W = 1$ Km^2, $\rho_0 = 100/W$, $k_0 = 40$, $k_1 = 13.03$, $\sigma = 3.5$.

As γ varies from 1 to 0, the area W remains constant while the domain $\mathcal{C}$ gets increasingly squeezed. The general trend suggests that the smaller is γ, the smaller is the level of connectivity. This is due to border effects: when S_2 becomes comparable with the transmission range, the connectivity area of the sinks is very likely to overstep the domain area, thus resulting in a decrement in the average number of connected sensors per sink. In particular, we expect this to be more appreciable for greater transmission ranges. In fact, from Fig. 4 we can observe that for $L_{\rm th} = 80$ dB ($TR_i \approx 21.54$ m), when γ ranges from 1 to 0.001 (S_2 ranging from 1000 m to 31.62 m) the loss in connectivity is only $\bar{q}(L_{\rm th} = 80 \text{ dB}; \gamma = 1) - \bar{q}(L_{\rm th} = 80 \text{ dB}; \gamma = 0.001) \approx 0.04$. Instead, for $L_{\rm th} = 100$ dB ($TR_i \approx 99.96$ m) and γ ranging as above, the loss in connectivity is no less than $\bar{q}(L_{\rm th} = 100 \text{ dB}; \gamma = 1) - \bar{q}(L_{\rm th} = 100 \text{ dB}; \gamma = 0.001) \approx 0.51$.

5.4.2 Composite Domain

Consider now the non-isolation probability for the composite domain of Figure 3. Assume $S_1^{(1)} = 850$ m, $S_2^{(1)} = 400$ m, $S_2^{(2)} = 150$ m, $S_1^{(3)} = 700$ m, $S_1^{(4)} = 400$ m, $S_2^{(4)} = 300$ m and the densities $\rho_{0,1} = 4.\text{E-}4$, $\rho_{0,2} = 3.\text{E-}3$, $\rho_{0,3} = 1.\text{E-}3$, $\rho_{0,4} = 6.\text{E-}4$.
From (27), the computation of $\bar{q}_{\rm p}$ is straightforward. In Figure 6 we report $\bar{q}_{\rm p}$, $\bar{q}_1$, $\bar{q}_2$, $\bar{q}_3$, $\bar{q}_4$.

As for $\bar{q}_{\mathrm{M}}$, set the origin in D and let (x_0, y_0) be a generic point in $\mathcal{C}'$. Accounting for the 4 different zones, the mean number of audible sinks from (x_0, y_0) is

$$\mu_{\mathrm{M}}(x_0, y_0) = \sum_{k=1}^{4} \rho_{0,k} \int_{\mathcal{C}'_k} C(||\mathbf{x} - \mathbf{x}_0||) d\mathbf{x} \tag{32}$$

$$\begin{aligned} &= \rho_{0,1} \int_{-x_0}^{S_1^{(1)}-x_0} \int_{S_1^{(4)}-y_0}^{S_1^{(4)}+S_2^{(1)}-y_0} C(\sqrt{(x-x_0)^2+(y-y_0)^2}) dy dx \\ &+ \rho_{0,2} \int_{S_1^{(1)}-x_0}^{S_1^{(1)}+S_2^{(2)}-x_0} \int_{S_1^{(4)}-y_0}^{S_1^{(4)}+S_2^{(1)}-y_0} C(\sqrt{(x-x_0)^2+(y-y_0)^2}) dy dx \\ &+ \rho_{0,3} \int_{S_2^{(4)}-x_0}^{S_2^{(4)}+S_1^{(3)}-x_0} \int_{-y_0}^{S_1^{(4)}-y_0} C(\sqrt{(x-x_0)^2+(y-y_0)^2}) dy dx \\ &+ \rho_{0,4} \int_{-x_0}^{S_2^{(4)}-x_0} \int_{-y_0}^{S_1^{(4)}-y_0} C(\sqrt{(x-x_0)^2+(y-y_0)^2}) dy dx, \end{aligned} \tag{33}$$

while the probabilities of non-isolation of the position (x_0, y_0) is obtained as

$$q_{\mathrm{M}}(x_0, y_0) = 1 - e^{-\mu_{\mathrm{M}}(x_0, y_0)}. \tag{34}$$

In Figure 5 $q_{\mathrm{M}}(x_0, y_0)$ is reported. Note that we have $q_{\mathrm{M}}(x_0, y_0) \neq 0$ on the boundaries, a fact that confirms that we are not introducing factitious border effects between different sub-domains. Note also that equations (32), (33) contain a double integral: this implies a greater computational complexity with respect to (19) employed in the Approach 1. On the other hand, (32) and (33) are exact (i.e., interactions among sub-domains $\mathcal{C}'_i$ are not neglected).
Now, accordingly to (25), the average probability $\overline{q}_{\mathrm{M}}$ that a sensor randomly chosen in $\mathcal{C}'$ is not isolated is

$$\overline{q}_{\mathrm{M}} = \mathbb{E}_{x_0, y_0}[q_{\mathrm{M}}(x_0, y_0)] = \int_0^{S_2^{(4)}+S_1^{(3)}} \int_0^{S_1^{(4)}+S_2^{(1)}} q_{\mathrm{M}}(x_0, y_0) dy_0 dx_0. \tag{35}$$

In Figure 6 we also plot $\bar{q}_{\mathrm{M}}$ as a function of L_{th} [dB]. It is possible to compare the non-isolation probabilities obtained through the two different approaches (bold curves): Approach 2, as said, accounts for interactions between sub-domains and thus does not introduce border effects that would be fake. This is the reason why we observe $\bar{q}_{\mathrm{M}} \geq \bar{q}_{\mathrm{P}}$ (i.e., the WSN performs better). Thus $\bar{q}_{\mathrm{P}}$ is a lower bound.

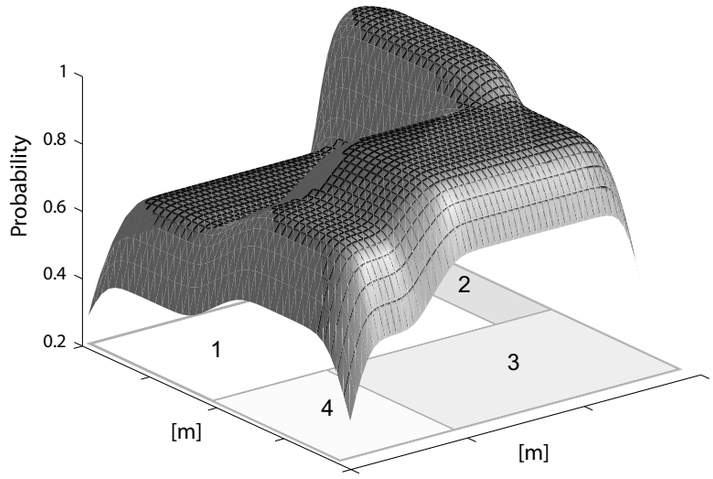

Fig. 5. $\bar{q}_{\mathrm{M}}(x_0, y_0)$ on the domain of Figure 3 obtained with $L_{th} = 90$ [dB], $k_0 = 40$, $k_1 = 13.03$, $\sigma = 3.5$.

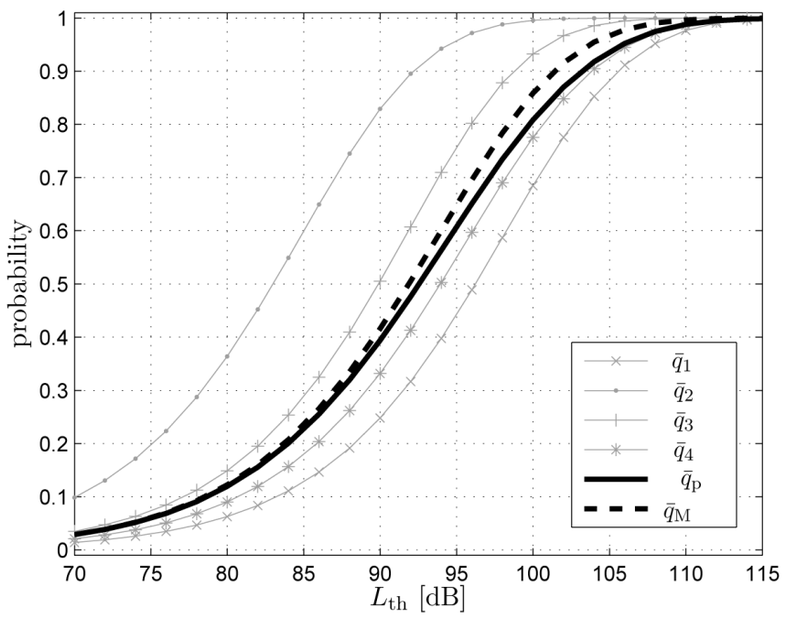

Fig. 6. Non-isolation probabilities referred to the scenario of Figure 3 obtained with $k_0 = 40$, $k_1 = 13.03$, $\sigma = 3.5$.

6. The IEEE 802.15.4 MAC protocol

When dealing with contention-based MAC protocols, there exists a certain probability that a node does not succeed in accessing the channel or in transmitting its packet correctly (i.e.,

without collisions). A single-sink scenario, where n 802.15.4 sensors transmit data to the sink through a direct link is accounted for, in this Section. We assume all sensor nodes are audible to the sink.
Both, Beacon- and Non Beacon-Enabled modes are considered. We assume that nodes transmit packets having a size, denoted as z, equal to $D \cdot 10$ bytes, where D is an integer parameter. We also assume that the size of the query packet is equal to 60 bytes.We denote as T the time needed for transmitting 10 bytes. Since a bit rate of 250 kbit/sec is used, $T = 320\mu sec$.
The Non Beacon-Enabled mode is based on CSMA/CA protocol to access the channel, whereas in the Beacon-Enabled case both contention-based and contention-free protocols, are implemented. In the latter case a superframe is defined, which starts with a packet denoted as Beacon (it coincides with the query packet in our scenario), and divided into two parts: inactive and active part. The active part is composed of the Contention Access Period (CAP), where a CSMA/CA protocol is used, and the Contention Free Period (CFP), where a maximum number of 7 Guaranteed Time Slots (GTSs) could be allocated to specific nodes (see Figure 7, below). The use if GTSs is optional.
The duration of the whole superframe and of its active part depends on the value of two integer parameters ranging from 0 to 14, called superframe order, denoted as SO, and beacon order, denoted as BO, with $BO \geq SO$. In particular, the interval of time between two successive Beacons, that is the query interval T_q in our scenario, is given by: $T_q = 16 \cdot 60 \cdot 2^{BO} \cdot T_s$, where $T_s = 16$ μsec is the symbol time. Instead, the duration of the active part, denoted as T_A, is given by: $T_A = 16 \cdot 60 \cdot 2^{SO} \cdot T_s$, where $60 \cdot 2^{SO} T_s$ is the slot size.
The inactive part of the superframe is generally used when tree-based or mesh topologies are applied; here, since we are dealing with star topologies, we set $SO = BO$ and $T_A = T_q$.
Each GTS must contain the packet to be transmitted and an inter-frame space equal to 40 T_s. This is, in fact, the minimum interval of time that must be guaranteed between the reception of two subsequent packets. The sink (PAN coordinator, in 802.15.4 jargon) may allocate up to seven GTSs; however, a sufficient portion of the CAP must remain for contention-based access. The minimum CAP size is 440 T_s. By varying packet size D and SO (i.e., the slot duration), the number of slots occupied by each GTS and the maximum number of GTSs that could be allocated to ensure a CAP larger than 440 T_s, will vary as well. As an example, if $D = 2$ and $SO = 0$, two slots are needed for a GTS, to contain the packet and the inter-frame space and a maximum number of 4 GTSs could be allocated. In case $SO = 2$, instead, each GTS will occupy one slot and seven Guaranteed Time Slots (GTSs) could be allocated. We denote as N_{GTS} the number of GTSs allocated.
We assume that in case a node does not succeed in accessing the channel by the end of the superframe (in the Beacon-Enabled case) or till reception of the subsequent query (in the Non Beacon-Enabled case), the packet will be lost.This implies that by increasing the superframe duration the success probability for a node will increase since the node will have more time to try to access the channel. Note that in the Beacon-Enabled case, T_q may assume only a finite set of values (depending on the values of BO); instead, in the Non Beacon-Enabled case T_q may assume any value. Note that, being $(120 + D) \cdot T$ the maximum delay with which a packet can be received by the sink Buratti & Verdone (2009) and having set the query size equal to 60 bytes, the sink should set $T_q \geq (126 + D) \cdot T$ to make sure all nodes have completed the CSMA/CA algorithm. In case lower values of T_q are set, a node may receive a new query while still trying to access the channel, this resulting in the loss of the old packet.
We parametrized the behavior of 802.15.4 MAC protocol by means of a function, $P_{MAC}(n)$, which returns the probability that a sensor node is successful in transmitting its packet when

$(n-1)$ more sensors are trying to do the same. We refer to Buratti & Verdone (2008; 2009) and Buratti (2009), Buratti (2010) for derivation and expression of $P_{MAC}(n)$ in Non Beacon- and Beacon-Enabled cases, respectively. A finite state transition diagram has been used to model sensor nodes states, in both cases Beacon- and Non Beacon-Enabled mode. Here we do not report equations for the sake of brevity. In these papers details on formulae are given and also a validation of the model against simulation is provided for $n \leq 50$ and different values of D.

6.1 Numerical results

Some examples of results obtained through the mathematical model developed are shown, with the aim of comparing those achieved with the two operation modes (i.e., Beacon- and Non Beacon-Enabled).

In Figures 8(a) $P_{MAC}(n)$ as functions of n for the Beacon-Enabled case, for different values of SO, with $D = 2$, is shown. The cases of no GTSs allocated and N_{GTS} equal to the maximum number of GTSs allocable, are considered. As explained above, this maximum number depends on the values of D and SO. As we can see, P_{MAC} decreases monotonically (for $n > 1$ when $N_{GTS} = 0$ and for $n > N_{GTS}$ when $N_{GTS} > 0$), by increasing n, since the number of sensors competing for the channel increases. Once we fix SO, by increasing N_{GTS}, P_{MAC} also increases, since less nodes have to compete for the channel. Moreover, once N_{GTS} is fixed, by increasing SO, P_{MAC} also grows, since the CAP size is greater and nodes have a larger amount of time to try to access the channel.

In Figure 8(b) $P_{MAC}(n)$ for different values of D and T_q, considering a Non Beacon-Enabled network, is shown. As we can see, a decrease of T_q, results in a decrement of P_{MAC}, since nodes have a smaller amount of time to access the channel.

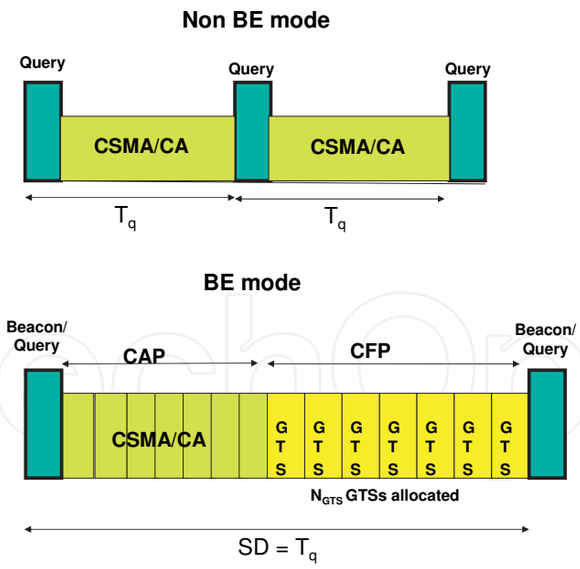

Fig. 7. Above part: The IEEE 802.15.4 Non Beacon-Enabled mode. Below part: The IEEE 802.15.4 Beacon-Enabled mode.

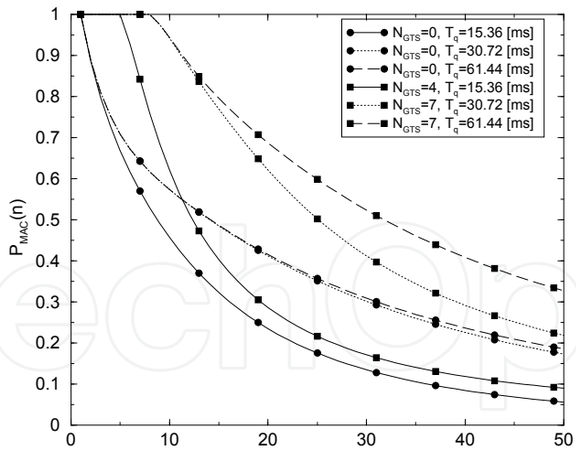

(a)

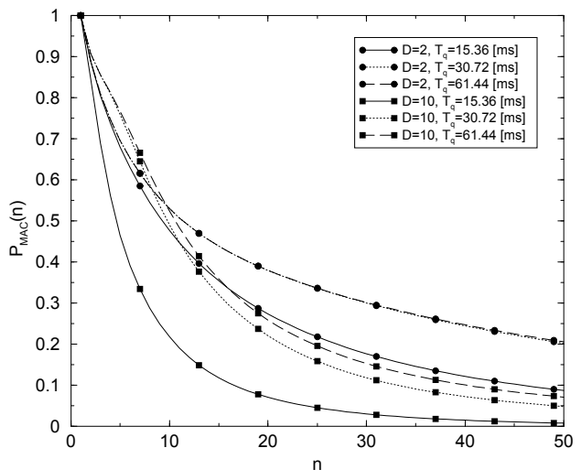

(b)

Fig. 8. (a): $P_{MAC}(n)$ as a function of n, in the Beacon-Enabled case, for different values of SO and N_{GTS}, having fixed $D = 2$. (b): $P_{MAC}(n)$ as a function of n, in the Non Beacon-Enabled case, for different values of T_q and D.

If we compare the above Figures, we notice that once the superframe duration is fixed, results are approximatively the same if no GTSs are allocated, whereas, there is a considerable increment of $P_{MAC}(n)$ in the Beacon-Enabled case when GTSs are allocated. Note that the cases $T_q = 15.36$ [ms], $T_q = 30.72$ [ms] and $T_q = 61.44$ [ms] correspond to $SO = 0$, 1 and 2, respectively.

7. Evaluation of the Area Throughput

The area throughput is mathematically derived through an intermediate step: first the probability of successful data transmission by an arbitrary sensor node, when k nodes are present in the monitored area, is considered. Then, the overall area throughput is evaluated based on this result.

7.1 Joint MAC/Connectivity Probability of Success

Let us consider an arbitrary sensor node that is located in the observed area A at a certain time instant. The aim is computing the probability that it can connect to one of the sinks deployed in A and successfully transmit its data sample to the infrastructure. Such an event is clearly related to connectivity issues (i.e., the sensor must employ an adequate transmitting power in order to reach the sink and not be isolated) and to MAC problems (i.e., the number of sensors which attempt at connecting to the same sink strongly affects the probability of successful transmission). For this reason, we define $P_{s|k}(x,y)$ as the probability of successful transmission conditioned on the overall number, k, of sensors present in the monitored area, which also depends on the position (x,y) of the sensor relative to a reference system with origin centered in A. This dependence is due to the well-known border effects in connectivity Bettstetter (2002).
In particular,

$$\begin{aligned} P_{s|k}(x,y) &= E_n[P_{MAC}(n) \cdot P_{CON}(x,y)] \\ &= E_n[P_{MAC}(n)] \cdot P_{CON}(x,y). \end{aligned} \tag{36}$$

where the impact of connectivity and MAC on the transmission of samples are separated. A packet will be successfully received by a sink if the sensor node is connected to at least one sink and if no MAC failures occur. The two terms that appear in (36) are now analysed.
$P_{CON}(x,y)$ represents the probability that the sensor is not isolated (i.e., it receives a sufficiently strong signal from at least one sink). This probability decreases as the sensor approaches the borders (border effects). P_{CON} for multi-sink single-hop WSNs, in bounded and unbounded regions, has been computed in the previous Sections. In particular, for unbounded regions, $P_{CON}(x,y) \simeq P_{CON}$, that is equal to q_∞, given by eq. (12). Whereas, when bounded regions are considered, $P_{CON}(x,y)$ is equal to $q(x,y)$ given by eq. (17).
Specifically, since the position of the sensor is in general unknown, $P_{s|k}(x,y)$ of (36) can be deconditioned as follows:

$$\begin{aligned} P_{s|k} &= E_{x,y}[P_{s|k}(x,y)] \\ &= E_{x,y}[P_{CON}(x,y)] \cdot E_n[P_{MAC}(n)]\,. \end{aligned} \tag{37}$$

$E_{x,y}[P_{CON}(x,y)]$ is equal to $\overline{q}$ given by, e.g., eq. (25) when a rectangular region is accounted for. When, instead border effects are negligible, $E_{x,y}[P_{CON}(x,y)] = E_{x,y}[P_{CON}] = P_{CON}$, given by eq. (12).
Given the channel model described in (2) (and following), the average connectivity area of the sensor, that is the average area in which the sinks audible to the given sensor are contained, can be defined as

$$A_{\sigma_s} = \pi e^{\frac{2(L_{\text{th}}-k_0)}{k1}} e^{\frac{2\sigma_s^2}{k_1^2}}\,. \tag{38}$$

In Fabbri & Verdone (2008) it is also shown that border effects are negligible when $A_{\sigma_s} < 0.1A$. In the following only this case will be accounted for. Thus we have

$$P_{CON}(x,y) \simeq P_{CON} = 1 - e^{-\mu_0}, \tag{39}$$

where $\mu_0 = \rho_0 A_{\sigma_s} = I A_{\sigma_s}/A$ is the mean number of audible sinks on an infinite plane from any position Orriss & Barton (2003), being $I = \rho_0 \cdot A$ the average number of sinks in A.
$P_{MAC}(n)$, $n \geq 1$, is the probability of successful transmission when $n-1$ interfering sensors are present introduced in Section 6 for the 802.15.4 MAC case.

In general, when CSMA-based MAC protocols are considered, $P_{MAC}(n)$ is a monotonic decreasing function of the number, n, of sensors which attempt to connect to the same serving sink. This number is in general a random variable in the range $[0, k]$. In fact, note that in (36) there is no explicit dependence on k, except for the fact that $n \leq k$ must hold. Moreover in our case we assume $1 \leq n \leq k$, as there is at least one sensor competing for access with probability P_{CON} (39).
Orriss et al. (2002) showed that the number of sensors uniformly distributed on an infinite plane that hear one particular sink as the one with the strongest signal power (i.e., the number of sensors competing for access to such sink), is Poisson distributed with mean

$$\bar{n} = \mu_s \frac{1 - e^{-\mu_0}}{\mu_0}, \tag{40}$$

with $\mu_s = \rho_s A_{\sigma_s}$ being the mean number of sensors that are audible by a given sink. Such a result is relevant toward our goal even though it was derived on the infinite plane. In fact, when border effects are negligible (i.e., $A_{\sigma_s} < 0.1A$) and k is large, n can still be considered Poisson distributed. The only two things that change are:

- n is upper bounded by k (i.e., the pdf is truncated)
- the density ρ_s is to be computed as the ratio k/A $[m^{-2}]$, thus yielding $\mu_s = k\frac{A_{\sigma_s}}{A}$.

Therefore, we assume $n \sim \text{Poisson}(\bar{n})$, with

$$\bar{n} = \bar{n}(k) = k\frac{A_{\sigma_s}}{A}\frac{1 - e^{-\mu_{sink}}}{\mu_{sink}} = k\frac{1 - e^{-IA_{\sigma_s}/A}}{I}. \tag{41}$$

Finally, by taking the average in (37) explicit and neglecting border effects (see (39)), we get

$$P_{s|k} = (1 - e^{-IA_{\sigma_s}/A}) \cdot \frac{1}{M} \sum_{n=1}^{k} P_{MAC}(n) \frac{\bar{n}^n e^{-\bar{n}}}{n!}, \tag{42}$$

where

$$M = \sum_{n=1}^{k} \frac{\bar{n}^n e^{-\bar{n}}}{n!} \tag{43}$$

is a normalizing factor.

7.2 Area Throughput

The amount of samples generated by the network as response to a given query is equal to the number of sensors, k, that are present and active when the query is received. As a consequence, the average number of data samples-per-query generated by the network is the mean number of sensors, $\bar{k}$, in the observed area.
Now denote by G the available area throughput, that is the average number of samples generated per unit of time, given by

$$G = \bar{k} \cdot f_q = \rho_s \cdot A \cdot \frac{1}{T_q} \text{ [samples/sec]}. \tag{44}$$

From (44) we have $\bar{k} = GT_q$.

The average amount of samples received by the infrastructure per unit of time (area throughput), S, is given by:

$$S = \sum_{k=0}^{+\infty} S(k) \cdot g_k \ \ [\text{samples/sec}], \tag{45}$$

where

$$S(k) = \frac{k}{T_q} P_{s|k}, \tag{46}$$

g_k as in (1) and $P_{s|k}$ as in (42).
Finally, by means of (42), (43) and (44), equation (45) may be rewritten as

$$\begin{aligned} S &= \frac{1 - e^{-IA_{\sigma_s}/A}}{T_q} \\ &\cdot \sum_{k=1}^{+\infty} \frac{\sum_{n=1}^{k} P_{MAC}(n) \frac{\bar{n}^n e^{-\bar{n}}}{n!}}{\sum_{n=1}^{k} \frac{\bar{n}^n e^{-\bar{n}}}{n!}} \cdot \frac{(GT_q)^k e^{-GT_q}}{(k-1)!}. \end{aligned} \tag{47}$$

7.3 Numerical Results

In this section the area throughput obtained with the two modalities Beacon- and Non Beacon-Enabled, considering different values of D, SO, N_{GTS}, T_q and different connectivity levels, is shown.

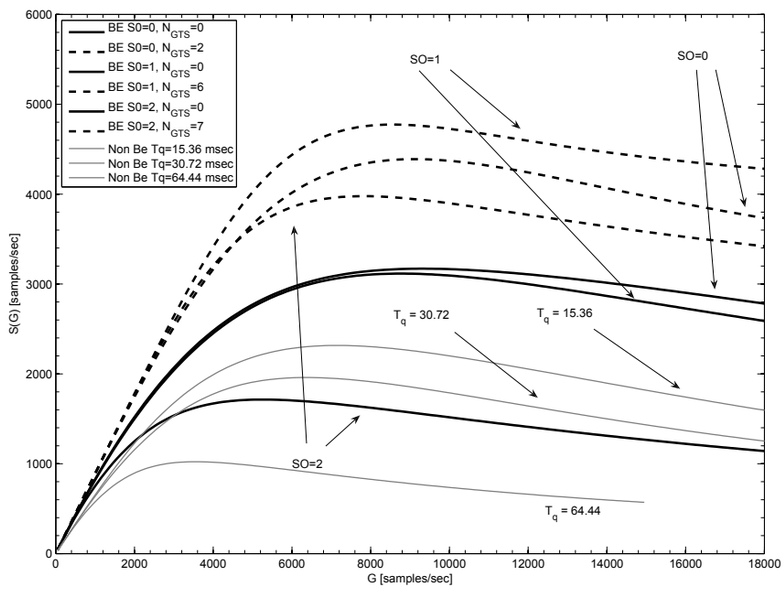

Fig. 9. S as a function of G, for the Beacon- and Non Beacon-Enabled cases, by varying SO, N_{GTS} and T_q, having fixed $D = 10$.

In Figure 9, S as a function of G, when varying SO, N_{GTS} and T_q for $D = 10$, is shown. The input parameters that we entered give a connection probability $P_{CON} = 0.89$. It can be noted

that, once SO is fixed (Beacon-Enabled case), an increase of N_{GTS} results in an increment of S, since P_{MAC} increases. Moreover, once N_{GTS} is fixed, there exists a value of SO maximising S. We can note that, a part for the case, Beacon-Enabled with GTSs allocated, an increase of SO results in a decrement of S. In fact, even though P_{MAC} gets greater the query interval increases and the number of samples per second received by the sink decreases. On the other hand, when the Beacon-Enabled mode is used and GTSs are allocated, the optimum value of SO is 1. This is due to the fact that, having large packets, when $SO = 0$ too many packets are lost, owing to the short duration of the superframe.
Concerning the Non Beacon-Enabled case, in both Figures it can be noted that, by decreasing T_q, S gets larger even though P_{MAC} decreases, since, once again, the MAC losses are balanced by larger values of f_q.

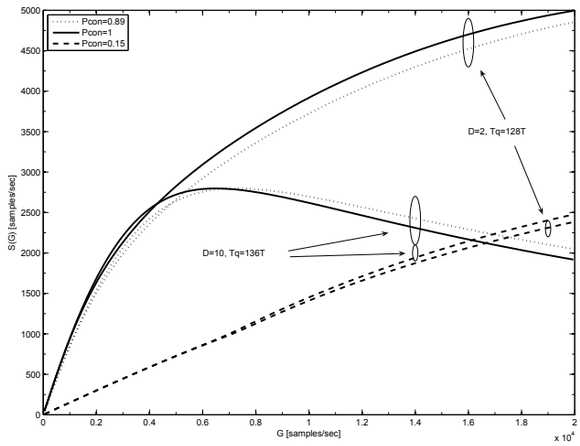

Fig. 10. S as a function of G, in the non beacon-enabled case, for different values of D and P_{CON}, having fixed T_q to the maximum delay.

Finally, we show the effects of connectivity on the area throughput. When P_{CON} is less than 1, only a fraction of the deployed nodes has a sink in its vicinity. In particular, an average number, $\bar{k} = P_{CON} G T_q / I$, of sensors compete for access at each sink. In Figure 10 we consider the non beacon-enabled case with $D = 2$, $T_q = 128\,T$ and $D = 10$, $T_q = 136\,T$. When $D = 10$, $T_q = 136\,T$, for high G the area throughput tends to decay, since packet collisions dominate. Hence, by moving from $P_{CON} = 1$ to $P_{CON} = 0.89$, we observe a slight improvement due to the fact that a smaller average number of sensors tries to connect to the same sink. Conversely, when $D = 2$, $T_q = 128\,T$, S is still increasing with G, then by moving from $P_{CON} = 1$ to $P_{CON} = 0.89$, we just reduce the useful traffic. Furthermore, when $P_{CON} = 0.15$, the available area throughput is very light, so that we are working in the region where $P_{MAC}(D = 2, T_q = 128T) < P_{MAC}(D = 10, T_q = 136\,T)$, resulting in a slightly better performance of the case with $D = 2$. Thus we conclude that the effect of lowering P_{CON} results in a stretch of the curves reported in the previous plots.

8. Acknowledgments

This work was supported by the European Commission in the framework of the FP7 Network of Excellence in Wireless Communications NEWCOM++ (contract n. 216715). Authors would like to thank Roberto Verdone for the fruitful discussions about the model.

9. List of acronyms

r.v. random variable

PAN Personal Area Network

CAP Contention Access Period

CFP Contention Free Period

CSMA carrier-sense multiple access

CSMA/CA carrier-sense multiple access with collision avoidance

GTS Guaranteed Time Slot

ISM industrial scientific medical

MAC medium access control

p.d.f. probability distribution function

PPP Poisson Point Process

PAN personal area network

WSN wireless sensor network

10. References

Bettstetter, C. (2002). On the minimum node degree and connectivity of a wireless multihop network, *Mobile Ad Hoc Networks and Comp.(Mobihoc), Proc. ACM Symp. on*.

Bettstetter, C. & Zangl, J. (2002). How to achieve a connected ad hoc network with homogeneous range assignment: an analytical study with consideration of border effects, *Mobile and Wireless Communications Network, 2002 4th International Workshop on*, pp. 125–129.

Bianchi, G. (2000). Performance analysis of the ieee 802.11 distributed coordination function, *IEEE Journal on Selected Areas of Communication (JSAC)* **18**: 535–547.

Bollobàs, B. (2001). *Random Graphs, Cambridge University Press, second ed.*

Buratti, C. (2009). A mathematical model for performance of ieee 802.15.4 beacon-enabled mode, *ACM IWCMC 2009*, Leipzig, Germany, June 21-24.

Buratti, C. (2010). Performance analysis of ieee 802.15.4 beacon-enabled mode., *Accepted for publication on IEEE Transactions on Vehicular Technology.*

Buratti, C. & Verdone, R. (2006). On the number of cluster heads minimizing the error rate for a wireless sensor network using a hierarchical topology over ieee 802.15.4, *Proc. of IEEE Int. Symp. on Personal, Indoor and MoRadio Communications, PIMRC 2006*, pp. 1–6.

Buratti, C. & Verdone, R. (2008). A mathematical model for performance analysis of ieee 802.15.4 non-beacon enabled mode, *Proc. IEEE European Wireless, EW2008*, Prague, Czech Republic.

Buratti, C. & Verdone, R. (2009). Performance analysis of ieee 802.15.4 non-beacon enabled mode.

Chen, Z., Lin, C., Wen, H. & Yin, H. (2007). An analytical model for evaluating ieee 802.15.4 csma/ca protocol in low rate wireless application, *Proc. IEEE AINAW 2007*.

Fabbri, F. & Verdone, R. (2008). Throughput analysis of an ieee 802.1lb multihop ad hoc network, *Proc. IEEE European Wireless, EW2008*, Prague, Czech.

Gardner, W. (1989). *Introduction to random processes: with applications to signals and systems*, second edn, McGraw Hill.

Kim, J. H. & Lee, J. K. (1999). Capture effects of wireless csma/ca protocols rayleigh and shadow fading channels, *IEEE Electronics Letters* **48**(4): 1277–1286.

Kim, T. O., Kim, H., Lee, J., Park, J. S. & Choi, B. D. (2006). Performance analysis of the ieee 802.15.4 with non beacon-enabled csma/ca in non-saturated contition, *International Conference on Embedded And Ubiquitous Computing, 2006. EUC 2006*, pp. 884–893.

Meester, R. & Roy, R. (1996). *Cambridge University Press, Cambridge UK*.

Miorandi, D. & Altman, E. (2005). Coverage and connectivity of ad hoc networks in presence of channel randomness, *Proc. of 24th Annual Joint Conference of the IEEE Computer and Communications Societies, INFOCOM 2005.*, Vol. 1, pp. 491–502.

Misic, J., Misic, V. B. & Shafi, S. (2004). Performance of ieee 802.15.4 beacon-enabled pan with uplink transmissions in non-saturation mode - access delay for finite buffers, *Proc. First International Conference on Broadband Networks, 2004. BroadNets 2004*, pp. 416–425.

Misic, J., Shafi, S. & Misic, V. B. (2005). The impact of mac parameters on the performance of 802.15.4 pan, *Elsevier Ad hoc Networks Journal* **3**: 509–528.

Misic, J., Shafi, S. & Misic, V. B. (2006). Maintaining reliability through activity management in an 802.15.4 sensor cluster, **3**: 779–788.

Orriss, J. & Barton, S. K. (2003). Probability distributions for the number of radio transceivers which can communicate with one another, **51**(4): 676–681.

Orriss, J., Phillips, A. & Barton, S. (1999). A statistical model for the spatial distribution of mobiles and base stations, *Proc. of IEEE Vehicular Technol. Conference, VTC 1999*, Vol. 1, pp. 19–22.

Orriss, J., Zanella, A., Verdone, R. & Barton, S. (2002). Probability distributions for the number of radio transceivers in a hot spot with an application to the evaluation of blocking probabilities, *IEEE Proc. of Personal, Indoor and Mobile Radio Communications, 2002*, Vol. 2.

Park, T., Kim, T., Choi, J., Choi, S. & Kwon, W. (2005). Throughput and energy consumption analysis of ieee 802.15.4 slotted csma/ca, *IEEE Electronics Letters* **41**: 1017–1019.

Penrose, M. D. (1993). On the spread-out limit for bond and continuum percolation, *Annals of Applied Probability* **3**: 253–276.

Penrose, M. D. (1999). On k-connectivity for a geometric random graph, *Random Structures and Algorithms* **15**: 145–164.

Penrose, M. D. & Pistztora, A. (1996). Large deviations for discrete and continous percolation, *Advances in Applied Probability* **28**: 29–52.

Pishro-Nik, Chan, K. & Fekri, F. (2004). On connectivity properties of large-scale sensor networks, *Sensor and Ad Hoc Communications and Networks, 2004. IEEE SECON04. First Annual IEEE Communications Society Conference on*, pp. 498–507.

Pollin, S., Ergen, M., Ergen, S., Bougard, B., der Pierre, L. V., Catthoor, F., Moerman, I., Bahai, A. & Varaiya, P. (2008). Performance analysis of slotted carrier sense ieee 802.15.4 medium access layer, **7**: 3359–3371.

Salbaroli, E. & Zanella, A. (2006). A statistical model for the evaluation of the distribution of the received power in ad hoc and wireless sensor networks, *Sensor and Ad Hoc Communications and Networks, SECON '06, 3rd Annual IEEE Communications Society on*, Vol. 3, pp. 756–760.

Santi, P. & Blough, D. M. (2003). The critical transmitting range for connectivity in sparse wireless ad hoc networks, **2**(1): 25–39.

Siripongwutikorn, P. (2006). Throughput analysis of an ieee 802.1lb multihop ad hoc network, *Proc. IEEE TENCON 2006*, pp. 1–4.

Stoyan, D., Kendall, W. S. & Mecke, J. (1995). *Stochastic Geometry and its Applications*.

Stuedi, P., Chinellato, O. & Alonso, G. (2005). Connectivity in the presence of shadowing in 802.11 ad hoc networks, *Proc. IEEE WCNC, 2005*.

Takagi, H. & Kleinrock, L. (1985). Throughput analysis for persistent csma systems, **33**(7): 627–638.

Verdone, R., Dardari, D., Mazzini, G. & Conti, A. (2008). *Wireless sensor and actuator networks*, Elsevier.

Vincze, Z., Vida, R. & Vidacs, A. (2007). Deploying multiple sinks in multi-hop wireless sensor networks, *Pervasive Services, IEEE International Conference on*, pp. 55–63.

Zdunek, K., Ucci, D. & Locicero, J. (1989). Throughput of nonpersistent inhibit sense multiple access with capture, *IEEE Electronics Letters* **25**(1): 30–31.

IntechOpen

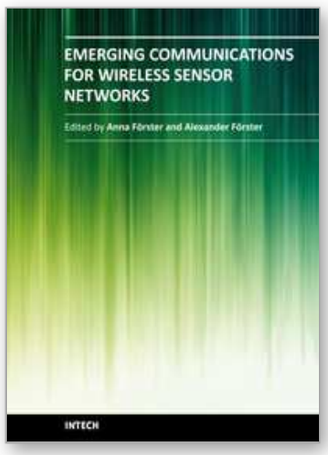

Emerging Communications for Wireless Sensor Networks

Edited by

ISBN 978-953-307-082-7
Hard cover, 270 pages
Publisher InTech
Published online 07, February, 2011
Published in print edition February, 2011

Wireless sensor networks are deployed in a rapidly increasing number of arenas, with uses ranging from healthcare monitoring to industrial and environmental safety, as well as new ubiquitous computing devices that are becoming ever more pervasive in our interconnected society. This book presents a range of exciting developments in software communication technologies including some novel applications, such as in high altitude systems, ground heat exchangers and body sensor networks. Authors from leading institutions on four continents present their latest findings in the spirit of exchanging information and stimulating discussion in the WSN community worldwide.

How to reference

In order to correctly reference this scholarly work, feel free to copy and paste the following:

Flavio Fabbri and Chiara Buratti (2011). Throughput Analysis of Wireless Sensor Networks via Evaluation of Connectivity and MAC Performance, Emerging Communications for Wireless Sensor Networks, (Ed.), ISBN: 978-953-307-082-7, InTech, Available from: http://www.intechopen.com/books/emerging-communications-for-wireless-sensor-networks/throughput-analysis-of-wireless-sensor-networks-via-evaluation-of-connectivity-and-mac-performance

INTECH
open science | open minds

InTech Europe
University Campus STeP Ri
Slavka Krautzeka 83/A
51000 Rijeka, Croatia
Phone: +385 (51) 770 447
Fax: +385 (51) 686 166
www.intechopen.com

InTech China
Unit 405, Office Block, Hotel Equatorial Shanghai
No.65, Yan An Road (West), Shanghai, 200040, China
中国上海市延安西路65号上海国际贵都大饭店办公楼405单元
Phone: +86-21-62489820
Fax: +86-21-62489821

IntechOpen